Electronic Supplementary Material (ESI) for CrystEngComm.

Supplementary information

Preparation of CL-20/TFAZ cocrystals under aqueous condition: balancing high performance and low sensitivity

Ning Liu,* Binghui Duan, Xianming Lu, Qian Zhang, Minghui Xu, Hongchang Mo and Bozhou Wang

Email: flackliu@sina.com

Table of Contents

1. X-ray crystallography

The CL-20/TFAZ cocrystal **1a** was obtained from the solution in isopropyl acetate at 20 °C. Crystal data, bond lengths, bond angles and dihedral angles of the data collection and refinement are given in Table S1, S2, and S3.

Table S1 Crystal data and structure refinement for CL-20/TFAZ cocrystal

CL-20/TFAZ cocrystal **1a**	
Empirical formula	$C_{12}H_7N_{19}O_{15}$
Formula weight	657.37
Temperature/K	296(2)
Crystal system	Monoclinic
Wavelength/Å	0.71073
Space group	$P2_1$
Unit cell dimensions/Å, º	a = 8.288 (2), α = 90
	b = 11.555 (3), β = 91.113 (6)
	c = 11.805 (3), γ = 90
Cell volume/Å^3	1130.3(5)
Z	2
ρ_{cal}/g cm^{-3}	1.932
μ/mm^{-1}	0.177
F(000)	664
Crystal size/mm	0.35 × 0.21 × 0.13
Crystal description	colorless needle
2θ range for data collection/°	2.46 to 25.10
Limiting indices	$-8 \le h \le 9$, $-13 \le k \le 13$, $-14 \le l \le 11$
Reflections collected	5723
Max. and min. transmission	0.9770 and 0.9399
Data/restraints/parameters	3885/1/416
Goodness-of-fit on F^2	0.985
Final R indexes [$I \ge 2\sigma$]	R_1 = 0.0566, wR_2 = 0.0787
R indexes [all data]	R_1 = 0.1199, wR_2 = 0.0993
Extinction coefficient	0.0045(8)
Largest diff. peak and hole/e Å^{-3}	0.234 and –0.230

Table S2 Bond lengths (Å) for CL-20/TFAZ cocrystal

N(1)-O(2)	1.218(6)	N(13)-C(7)	1.293(6)
N(1)-O(1)	1.226(6)	N(13)-O(13)	1.385(6)
N(1)-N(2)	1.361(7)	N(14)-C(8)	1.300(6)
N(2)-C(4)	1.449(7)	N(14)-O(13)	1.365(6)
N(2)-C(1)	1.457(7)	N(15)-C(9)	1.300(6)
N(3)-O(4)	1.198(6)	N(15)-O(15)	1.378(5)
N(3)-O(3)	1.213(6)	N(16)-C(10)	1.295(6)
N(3)-N(4)	1.408(7)	N(16)-O(15)	1.384(5)
N(4)-C(2)	1.432(6)	N(17)-C(11)	1.299(6)
N(4)-C(1)	1.437(6)	N(17)-O(14)	1.369(5)
N(5)-O(5)	1.221(6)	N(18)-C(12)	1.298(6)
N(5)-O(6)	1.223(6)	N(18)-O(14)	1.389(5)
N(5)-N(6)	1.450(6)	N(19)-C(7)	1.360(6)
N(6)-C(3)	1.471(7)	N(19)-C(12)	1.369(6)
N(6)-C(2)	1.480(6)	N(19)-H(19)	0.86
N(7)-O(8)	1.202(6)	C(1)-C(5)	1.582(6)
N(7)-O(7)	1.208(6)	C(1)-H(1)	0.98
N(7)-N(8)	1.423(6)	C(2)-C(6)	1.580(7)
N(8)-C(4)	1.472(7)	C(2)-H(2)	0.98
N(8)-C(5)	1.477(7)	C(3)-C(4)	1.586(6)
N(9)-O(10)	1.208(6)	C(3)-H(3)	0.98
N(9)-O(9)	1.222(6)	C(4)-H(4)	0.98
N(9)-N(10)	1.394(7)	C(5)-H(5)	0.98
N(10)-C(6)	1.438(7)	C(6)-H(6)	0.98
N(10)-C(5)	1.452(7)	C(7)-C(8)	1.427(7)
N(11)-O(12)	1.210(6)	C(8)-C(9)	1.465(7)
N(11)-O(11)	1.215(6)	C(9)-C(10)	1.400(6)
N(11)-N(12)	1.391(6)	C(10)-C(11)	1.448(6)
N(12)-C(3)	1.439(7)	C(11)-C(12)	1.412(7)
N(12)-C(6)	1.458(7)	N(13)-C(7)	1.293(6)

Table S3 Bond angles (º) for CL-20/TFAZ cocrystal

O(2)-N(1)-O(1)	127.0(6)	N(4)-C(1)-H(1)	111.5
O(2)-N(1)-N(2)	116.9(6)	N(2)-C(1)-H(1)	111.5
O(1)-N(1)-N(2)	116.1(6)	C(5)-C(1)-H(1)	111.5
N(1)-N(2)-C(4)	120.5(5)	N(4)-C(2)-N(6)	108.8(5)
N(1)-N(2)-C(1)	121.5(5)	N(4)-C(2)-C(6)	107.9(5)
C(4)-N(2)-C(1)	111.5(4)	N(6)-C(2)-C(6)	104.9(5)
O(4)-N(3)-O(3)	126.9(6)	N(4)-C(2)-H(2)	111.7
O(4)-N(3)-N(4)	115.9(6)	N(6)-C(2)-H(2)	111.7
O(3)-N(3)-N(4)	117.2(5)	C(6)-C(2)-H(2)	111.7
N(3)-N(4)-C(2)	118.8(5)	N(12)-C(3)-N(6)	104.9(4)
N(3)-N(4)-C(1)	120.9(5)	N(12)-C(3)-C(4)	110.2(5)
C(2)-N(4)-C(1)	118.7(5)	N(6)-C(3)-C(4)	106.7(4)
O(5)-N(5)-O(6)	128.5(5)	N(12)-C(3)-H(3)	111.6
O(5)-N(5)-N(6)	115.0(5)	N(6)-C(3)-H(3)	111.6
O(6)-N(5)-N(6)	116.2(5)	C(4)-C(3)-H(3)	111.6
N(5)-N(6)-C(3)	115.7(4)	N(2)-C(4)-N(8)	99.4(4)
N(5)-N(6)-C(2)	113.7(4)	N(2)-C(4)-C(3)	113.3(4)
C(3)-N(6)-C(2)	106.7(4)	N(8)-C(4)-C(3)	108.2(4)
O(8)-N(7)-O(7)	128.3(5)	N(2)-C(4)-H(4)	111.8
O(8)-N(7)-N(8)	115.4(5)	N(8)-C(4)-H(4)	111.8
O(7)-N(7)-N(8)	116.1(5)	C(3)-C(4)-H(4)	111.8
N(7)-N(8)-C(4)	116.0(4)	N(10)-C(5)-N(8)	109.8(5)
N(7)-N(8)-C(5)	116.8(5)	N(10)-C(5)-C(1)	107.3(5)
C(4)-N(8)-C(5)	108.2(4)	N(8)-C(5)-C(1)	104.9(5)
O(10)-N(9)-O(9)	126.7(6)	N(10)-C(5)-H(5)	111.5
O(10)-N(9)-N(10)	116.4(5)	N(8)-C(5)-H(5)	111.5
O(9)-N(9)-N(10)	116.7(5)	C(1)-C(5)-H(5)	111.5
N(9)-N(10)-C(6)	116.7(5)	N(10)-C(6)-N(12)	111.8(5)
N(9)-N(10)-C(5)	117.6(5)	N(10)-C(6)-C(2)	108.3(5)
C(6)-N(10)-C(5)	117.3(5)	N(12)-C(6)-C(2)	103.7(5)
O(12)-N(11)-O(11)	127.7(6)	N(10)-C(6)-H(6)	110.9
O(12)-N(11)-N(12)	117.7(6)	N(12)-C(6)-H(6)	110.9
O(11)-N(11)-N(12)	114.5(6)	C(2)-C(6)-H(6)	110.9
N(11)-N(12)-C(3)	120.0(5)	N(13)-C(7)-N(19)	120.8(5)
N(11)-N(12)-C(6)	120.7(5)	N(13)-C(7)-C(8)	108.7(5)
C(3)-N(12)-C(6)	108.7(5)	N(19)-C(7)-C(8)	130.6(5)
C(7)-N(13)-O(13)	105.6(5)	N(14)-C(8)-C(7)	109.1(5)
C(8)-N(14)-O(13)	105.6(4)	N(14)-C(8)-C(9)	122.5(5)
C(9)-N(15)-O(15)	104.3(4)	C(7)-C(8)-C(9)	128.4(5)
C(10)-N(16)-O(15)	104.5(4)	N(15)-C(9)-C(10)	109.9(4)
C(11)-N(17)-O(14)	105.9(4)	N(15)-C(9)-C(8)	123.4(5)
C(12)-N(18)-O(14)	104.1(5)	C(10)-C(9)-C(8)	126.6(4)
C(7)-N(19)-C(12)	127.5(5)	N(16)-C(10)-C(9)	109.8(5)

C(7)-N(19)-H(19)	116.2	N(16)-C(10)-C(11)	123.0(5)
C(12)-N(19)-H(19)	116.2	C(9)-C(10)-C(11)	127.2(4)
N(14)-O(13)-N(13)	111.0(4)	N(17)-C(11)-C(12)	108.4(5)
N(17)-O(14)-N(18)	111.1(4)	N(17)-C(11)-C(10)	122.7(5)
N(15)-O(15)-N(16)	111.5(4)	C(12)-C(11)-C(10)	128.9(5)
N(4)-C(1)-N(2)	113.0(5)	N(18)-C(12)-N(19)	118.9(5)
N(4)-C(1)-C(5)	108.5(5)	N(18)-C(12)-C(11)	110.4(5)
N(2)-C(1)-C(5)	100.5(5)	N(19)-C(12)-C(11)	130.6(5)

Table S4 Torsion angles (º) for CL-20/TFAZ cocrystal

O(2)-N(1)-N(2)-C(4)	-162.7(5)	N(6)-C(3)-C(4)-N(2)	-4.9(6)
O(1)-N(1)-N(2)-C(4)	18.8(7)	N(12)-C(3)-C(4)-N(8)	-0.8(6)
O(2)-N(1)-N(2)-C(1)	-13.3(8)	N(6)-C(3)-C(4)-N(8)	-114.1(5)
O(1)-N(1)-N(2)-C(1)	168.3(5)	N(9)-N(10)-C(5)-N(8)	-92.2(6)
O(4)-N(3)-N(4)-C(2)	-7.7(9)	C(6)-N(10)-C(5)-N(8)	55.0(6)
O(3)-N(3)-N(4)-C(2)	175.2(5)	N(9)-N(10)-C(5)-C(1)	154.4(5)
O(4)-N(3)-N(4)-C(1)	-173.4(6)	C(6)-N(10)-C(5)-C(1)	-58.5(7)
O(3)-N(3)-N(4)-C(1)	9.5(9)	N(7)-N(8)-C(5)-N(10)	132.2(5)
O(5)-N(5)-N(6)-C(3)	-164.7(5)	C(4)-N(8)-C(5)-N(10)	-94.6(5)
O(6)-N(5)-N(6)-C(3)	20.8(7)	N(7)-N(8)-C(5)-C(1)	-112.8(5)
O(5)-N(5)-N(6)-C(2)	-40.7(7)	C(4)-N(8)-C(5)-C(1)	20.4(6)
O(6)-N(5)-N(6)-C(2)	144.8(5)	N(4)-C(1)-C(5)-N(10)	1.7(7)
O(8)-N(7)-N(8)-C(4)	-154.9(5)	N(2)-C(1)-C(5)-N(10)	120.4(5)
O(7)-N(7)-N(8)-C(4)	29.5(7)	N(4)-C(1)-C(5)-N(8)	-115.0(5)
O(8)-N(7)-N(8)-C(5)	-25.4(7)	N(2)-C(1)-C(5)-N(8)	3.7(7)
O(7)-N(7)-N(8)-C(5)	159.0(5)	N(9)-N(10)-C(6)-N(12)	91.9(6)
O(10)-N(9)-N(10)-C(6)	25.7(7)	C(5)-N(10)-C(6)-N(12)	-55.5(6)
O(9)-N(9)-N(10)-C(6)	-159.7(6)	N(9)-N(10)-C(6)-C(2)	-154.4(5)
O(10)-N(9)-N(10)-C(5)	173.0(6)	C(5)-N(10)-C(6)-C(2)	58.2(7)
O(9)-N(9)-N(10)-C(5)	-12.3(8)	N(11)-N(12)-C(6)-N(10)	-121.1(6)
O(12)-N(11)-N(12)-C(3)	-12.7(9)	C(3)-N(12)-C(6)-N(10)	94.3(5)
O(11)-N(11)-N(12)-C(3)	171.4(5)	N(11)-N(12)-C(6)-C(2)	122.5(6)
O(12)-N(11)-N(12)-C(6)	-153.4(6)	C(3)-N(12)-C(6)-C(2)	-22.2(6)
O(11)-N(11)-N(12)-C(6)	30.7(8)	N(4)-C(2)-C(6)-N(10)	-0.8(7)
C(8)-N(14)-O(13)-N(13)	-0.1(6)	N(6)-C(2)-C(6)-N(10)	-116.6(5)
C(7)-N(13)-O(13)-N(14)	-0.6(6)	N(4)-C(2)-C(6)-N(12)	118.1(5)
C(11)-N(17)-O(14)-N(18)	-0.5(8)	N(6)-C(2)-C(6)-N(12)	2.3(7)
C(12)-N(18)-O(14)-N(17)	0.9(8)	O(13)-N(13)-C(7)-N(19)	-179.3(5)
C(9)-N(15)-O(15)-N(16)	0.2(8)	O(13)-N(13)-C(7)-C(8)	0.9(6)
C(10)-N(16)-O(15)-N(15)	0.4(8)	C(12)-N(19)-C(7)-N(13)	-179.0(6)
N(3)-N(4)-C(1)-N(2)	111.2(6)	C(12)-N(19)-C(7)-C(8)	0.8(11)
C(2)-N(4)-C(1)-N(2)	-54.6(7)	O(13)-N(14)-C(8)-C(7)	0.6(6)
N(3)-N(4)-C(1)-C(5)	-138.3(6)	O(13)-N(14)-C(8)-C(9)	-177.8(5)
C(2)-N(4)-C(1)-C(5)	55.9(7)	N(13)-C(7)-C(8)-N(14)	-1.0(7)
N(1)-N(2)-C(1)-N(4)	-64.2(6)	N(19)-C(7)-C(8)-N(14)	179.2(6)
C(4)-N(2)-C(1)-N(4)	87.7(5)	N(13)-C(7)-C(8)-C(9)	177.2(6)
N(1)-N(2)-C(1)-C(5)	-179.6(5)	N(19)-C(7)-C(8)-C(9)	-2.5(11)
C(4)-N(2)-C(1)-C(5)	-27.8(6)	O(15)-N(15)-C(9)-C(10)	-0.7(8)
N(3)-N(4)-C(2)-N(6)	-109.2(6)	O(15)-N(15)-C(9)-C(8)	177.3(6)
C(1)-N(4)-C(2)-N(6)	56.9(6)	N(14)-C(8)-C(9)-N(15)	0.3(10)
N(3)-N(4)-C(2)-C(6)	137.6(6)	C(7)-C(8)-C(9)-N(15)	-177.7(6)
C(1)-N(4)-C(2)-C(6)	-56.4(7)	N(14)-C(8)-C(9)-C(10)	178.0(6)
N(5)-N(6)-C(2)-N(4)	133.7(5)	C(7)-C(8)-C(9)-C(10)	-0.1(11)

C(3)-N(6)-C(2)-N(4)	-97.6(5)	O(15)-N(16)-C(10)-C(9)	-0.8(8)
N(5)-N(6)-C(2)-C(6)	-111.1(5)	O(15)-N(16)-C(10)-C(11)	178.5(6)
C(3)-N(6)-C(2)-C(6)	17.6(6)	N(15)-C(9)-C(10)-N(16)	1.0(9)
N(11)-N(12)-C(3)-N(6)	-111.1(5)	C(8)-C(9)-C(10)-N(16)	-177.0(6)
C(6)-N(12)-C(3)-N(6)	33.9(5)	N(15)-C(9)-C(10)-C(11)	-178.3(7)
N(11)-N(12)-C(3)-C(4)	134.5(5)	C(8)-C(9)-C(10)-C(11)	3.8(12)
C(6)-N(12)-C(3)-C(4)	-80.6(6)	O(14)-N(17)-C(11)-C(12)	-0.2(7)
N(5)-N(6)-C(3)-N(12)	96.0(5)	O(14)-N(17)-C(11)-C(10)	-180.0(6)
C(2)-N(6)-C(3)-N(12)	-31.5(5)	N(16)-C(10)-C(11)-N(17)	-3.2(11)
N(5)-N(6)-C(3)-C(4)	-147.1(4)	C(9)-C(10)-C(11)-N(17)	175.9(7)
C(2)-N(6)-C(3)-C(4)	85.4(5)	N(16)-C(10)-C(11)-C(12)	177.0(7)
N(1)-N(2)-C(4)-N(8)	-167.6(5)	C(9)-C(10)-C(11)-C(12)	-3.8(12)
C(1)-N(2)-C(4)-N(8)	40.2(5)	O(14)-N(18)-C(12)-N(19)	179.3(6)
N(1)-N(2)-C(4)-C(3)	77.9(6)	O(14)-N(18)-C(12)-C(11)	-1.0(8)
C(1)-N(2)-C(4)-C(3)	-74.4(6)	C(7)-N(19)-C(12)-N(18)	-178.9(7)
N(7)-N(8)-C(4)-N(2)	97.8(5)	C(7)-N(19)-C(12)-C(11)	1.5(12)
C(5)-N(8)-C(4)-N(2)	-35.7(5)	N(17)-C(11)-C(12)-N(18)	0.8(8)
N(7)-N(8)-C(4)-C(3)	-143.8(4)	C(10)-C(11)-C(12)-N(18)	-179.4(7)
C(5)-N(8)-C(4)-C(3)	82.7(5)	N(17)-C(11)-C(12)-N(19)	-179.6(7)
N(12)-C(3)-C(4)-N(2)	108.4(6)	C(10)-C(11)-C(12)-N(19)	0.2(13)

2. Computational details

Computations were performed with the Gaussian 09 (Revision B. 01) suite of programs.[1] Geometry optimization was performed with the hybrid meta-exchange correlation functional M062x at 6-311+G (d,p) level. The isodesmic reaction used for the prediction of gas-phase heats of formation (HOF) of CL-20, TFAZ and CL-20/TFAZ cocrystal are shown in Scheme S1. The experimental HOF of the reference compounds used in the isodesmic reactions are listed in Table S5.

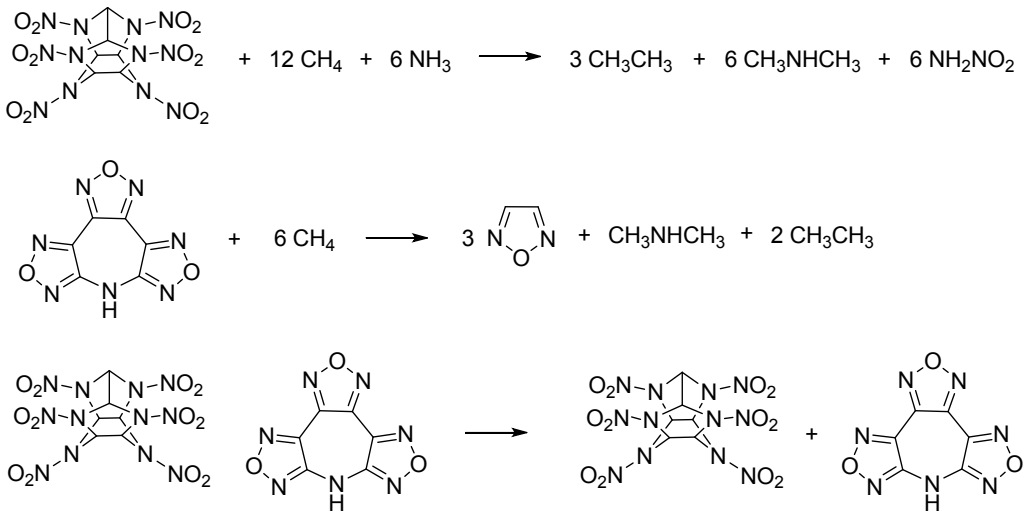

Scheme S1 Isodesmic reactions used to obtain the HOFs of CL-20/TFAZ cocrystal and co-formers at 298K

Table S5 Experimental gas-phase heats of formation for reference compounds at 298 K[2,3]

Compd.	$\Delta H_{f,gas}$ /kJ mol^{-1}
CH_4	–74.6
NH_3	–46.1
CH_3CH_3	–84.0
CH_3NHCH_3	–18.8
NH_2NO_2	–3.9
furazan	196.27

For the isodesmic reaction, the heat of reaction (ΔH_{298K}) is calculated from Eq. (1):[4]

$$\Delta H_{298K} = \Delta E_{298K} + \Delta(PV) = \Delta E_0 + \Delta ZPE + \Delta H_T + \Delta nRT \quad (1)$$

where ΔE_0 is the change in total energy between the products and the reactants at 0 K; ΔZPE is the difference between the zero-point energies of the products and the reactants at 0 K; ΔH_T is thermal correction from 0 to 298 K. The $\Delta(PV)$ term in Eq. (3) equals ΔnRT for the reactions of ideal gas. For the isodesmic reactions, Δn=0, so $\Delta(PV)$=0.

Furthermore, the solid-state HOF ($\Delta H_{f,solid}$) can be calculated by Eq. (2):

$$\Delta H_{f,solid} = \Delta H_{f,gas} - \Delta H_{sub} \quad (2)$$

Hirshfeld surface is constructed based on the electron distribution, calculated as the sum of spherical atom electron densities.[5] The normalized contact distance (d_{norm}) can be determined by Eq. (3):[6]

$$d_{norm} = \frac{d_i - r_i^{vdW}}{r_i^{vdW}} + \frac{d_e - r_e^{vdW}}{r_e^{vdW}} \quad (3)$$

Where d_i and d_e are the distances from the Hirshfeld surface to the nearest atoms inside and outside the surface, r_i^{vdW} and r_e^{vdW} denote the van der Waals radii of the appropriate atoms interior and exterior to the surface, respectively. All the Hirshfeld surfaces and their 2D fingerprint plots were created with Crystal Explorer 3.1.[7]

3. High performance liquid chromatography (HPLC) analysis

The HPLC analysis for CL-20/TFAZ cocrystal (**1a** and **1b**) was performed by Shimadzu LC-2010A apparatus by using acetone as mobile phase. The chromatogram and corresponding parameters were presented in Fig. S1 and Table S6, respectively.

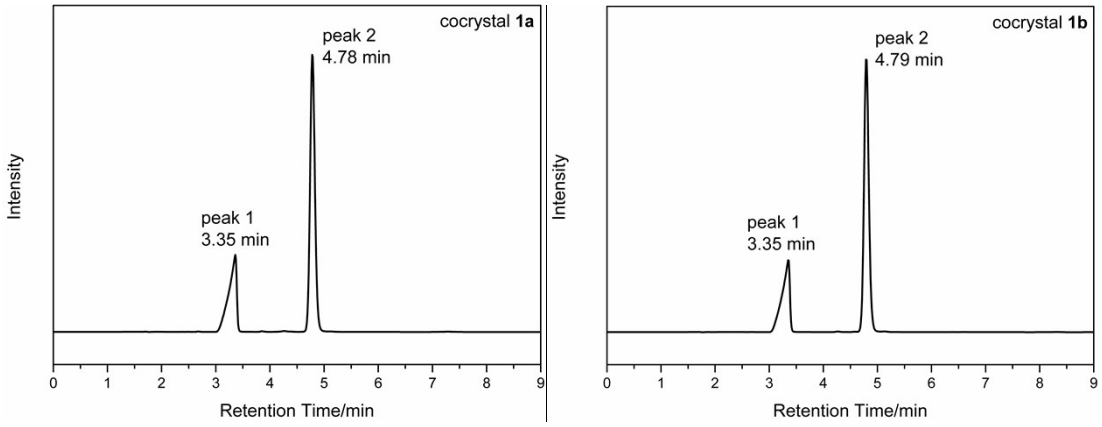

(a) (b)

Fig. S1 HPLC chromatogram of CL-20/TFAZ cocrystal: (a) **1a**; (b) **1b**

Table S6 The peak area and mass percentage of CL-20/TFAZ cocrystal

cocrystal **1a**				cocrystal **1b**			
peak	compound	area	mass/%	peak	compound	area	mass/%
1	TFAZ	2610576	33.24	1	TFAZ	2639805	33.17
2	CL-20	5243142	66.76	2	CL-20	5318606	66.83

References

1 M. J. Frisch, G. W. Trucks, H. B. Schlegel, G. E. Scuseria, M. A. Robb, J. R. Cheeseman, G. Scalmani, V. Barone, B. Mennucci, G. A. Petersson, H. Nakatsuji, M. Caricato, X. Li, H. P. Hratchian, A. F. Izmaylov, J. Bloino, G. Zheng, J. L. Sonnenberg, M. Hada, M. Ehara, K. Toyota, R. Fukuda, J. Hasegawa, M. Ishida, T. Nakajima, Y. Honda, O. Kitao, H. Nakai, T. Vreven Jr., J. A. Montgomery, J. E. Peralta, F. Ogliaro, M. Bearpark, J. J. Heyd, E. Brothers, K. N. Kudin, V. N. Staroverov, R. Kobayashi, J. Normand, K. Raghavachari, A. Rendell, J. C. Burant, S. S. Iyengar, J. Tomasi, M. Cossi, N.

Rega, J. M. Millam, M. Klene, J. E. Knox, J. B. Cross, V. Bakken, C. Adamo, J. Jaramillo, R. Gomperts, R. E. Stratmann, O. A. Yazyev, A. J. Austin, R. Cammi, C. Pomelli, J. W. Ochterski, R. L. Martin, K. Morokuma, V. G. Zakrzewski, G. A. Voth, P. Salvador, J. J. Dannenberg, S. Dapprich, A. D. Daniels, O. Farkas, J. B. Foresman, J. V. Ortiz, J. Cioslowski and D. J. Fox, Gaussian 09, Revision B. 01, Gaussian, Inc, Wallingford, CT, USA, 2009.

2 J. A. Dean, *LANGE'S Handbook of Chemistry, 15th ed.*, McGraw-Hill Book Co., New York, 1999.

3 H. Y. Afeefy, J. F. Liebman and S. E. Stein, Neutral thermochemical data, in: P.J. Linstrom, W.G. Mallard (Eds.), NIST Chemistry Web Book, NIST Standard Reference Database Number 69, National Institute of Standards and Technology, Gaithersburg, MD, 2000. <http://webbook.nist.gov>.

4 P.-Y. Chen, L. Zhang, S.-G. Zhu and G.-B. Cheng, *Can. J. Chem.*, 2015, **93**, 632.

5 J. W. Cui, Y. Q. Zhao, Z. C. Hao and G. H. Cui, *Res. Chem. Intermed.*, 2017, **44**, 721–738.

6 M. Nikpour, M. Mirzaei, Y. G. Chen, A. A. Kaju and M. Bakavoli, *Inorg. Chem. Commun.*, 2009, **12**, 879–882.

7 S. K. Wolff, D. J. Grimwood, J. J. McKinnon, D. Jayatilaka and M. A. Spackman, *Crystal Explorer 3.1*, University of Western Australia, Perth, Australia, 2009.